

Emergent Expansion Cosmology (EEC): A Thermodynamic Closure for the Backreaction Problem and its Background-Level Observational Confrontation

Ismail Khan

Independent Researcher,

Mardan, Pakistan

ismailkhan.mcs@gmail.com

DOI: **10.5281/zenodo.20257255**

ORCID: 0009-0005-7485-8880

Preprint - Version 7

May 2026

Version Note

EEC v7 supersedes v6 with one methodological correction and its consequences.

The single methodological change is the replacement of the Planck compressed parameter $\omega_m = 0.1430 \pm 0.0011$, previously used as a prior in v6. This parameter is derived by fitting Λ CDM to CMB data and therefore implicitly encodes Λ CDM geometry through the comoving distance to last scattering, $\chi(z_*)$. Since EEC predicts a different expansion history, this prior is geometrically inconsistent with the EEC framework. In v7, it is replaced by the model-independent Planck acoustic scale $\theta_* = 0.010409 \pm 0.000006$, measured directly from the angular positions of the CMB acoustic peaks without assuming a cosmological model and evaluated self-consistently within EEC geometry. This correction resolves the 5.4σ θ_* tension present in v6 to $+0.27\sigma$, while correspondingly shifting the best-fit cosmological parameters.

Three additional dataset corrections were implemented in v7:

- ω_b updated to 0.02233 using the correct BBN determination from Cooke, Pettini & Steidel (2016, *ApJ* 830, 148).
- θ_* uncertainty corrected from 0.000031 to 0.000006 using the model-independent Planck Table 2 value.
- BOSS DR12 covariance extended to the full 9×9 matrix including the $D_M - f\sigma_8$ and $D_H - f\sigma_8$ cross-correlation terms following Alam et al. (2017, Table 3).

No changes were made to the EEC equations, the stiffness function $\kappa(\rho_m) = \kappa_0 x e^{-x}$, the halo transition redshift $z_{\text{halo}} = 1.1$, the growth solver, or any theoretical section.

Note on Ω_c : Throughout this paper, Ω_c denotes the EEC characteristic density parameter defined as $\Omega_c \equiv \Omega_m(1 + z_{\text{halo}})^3 = \rho_c/\rho_{\text{crit}}$ where ρ_c is the matter density at the epoch of peak stiffness $z_{\text{halo}} = 1.1$. Because the Universe was denser in the past, $\rho_c = 9.261 \times \rho_m(z = 0)$, and therefore $\Omega_c = 9.261 \times \Omega_m \approx 2.95$. This quantity is not a density fraction and is not bounded by unity. It has no counterpart in Λ CDM, where all Ω -parameters denote present-day density fractions summing to unity. The result $\Omega_c > 1$ is

therefore a required consequence of the EEC framework rather than a numerical inconsistency.

Abstract

We propose a thermodynamically motivated closure model for the Buchert backreaction equations of general relativity, in which the kinematic backreaction term is associated with the non-equilibrium free energy of the matter distribution evaluated at a coarse-grained nonlinear scale R_s .

The central hypothesis is that the variance of density fluctuations, generated through gravitational collapse and structure formation, produces an effective backreaction contribution proportional to $\sigma^4(R_s)$, with a density-dependent coefficient motivated by Press–Schechter statistics.

Within this framework, the non-equilibrium free energy density is modeled as

$$f_{\text{neq}} = \frac{\kappa_0}{2} \left(\frac{\rho_m}{\rho_c} \right) e^{-\rho_m/\rho_c} \xi^2$$

where $\xi = \sigma^2(R_s, t)$ denotes the variance of density fluctuations at the coarse-graining scale. The stiffness function

$$\kappa(\rho_m) = \kappa_0 \left(\frac{\rho_m}{\rho_c} \right) e^{-\rho_m/\rho_c}$$

is adopted as a physically motivated ansatz consistent with the Coleman–Gurtin thermodynamic formalism and with the qualitative behavior expected from Press–Schechter collapse statistics; a rigorous first-principles derivation remains an open theoretical task.

Within the adopted pressure prescription, the effective equation of state satisfies

$$w_{\text{neq}} = -1$$

at $\rho_m = \rho_c$ for any admissible stiffness function exhibiting a maximum at this characteristic density scale.

The framework is constructed to satisfy the Bianchi identity at the homogeneous background level, while the second law of thermodynamics emerges as a structural consequence of the dynamics during the epoch of active structure formation. At the level of linear perturbations, the internal variable obeys

$$\delta\xi = 0$$

implying that no additional propagating degrees of freedom are introduced. This leads to a modified Poisson equation characterized by a redshift-dependent effective coupling $\mu(z)$, while preserving a vanishing gravitational slip parameter,

$$\eta = 0$$

where $\eta \equiv \Phi/\Psi - 1$, so that $\eta = 0$ corresponds to the absence of gravitational slip ($\Phi = \Psi$).

Within the Buchert formalism, the leading-order backreaction contribution remains negative and scales as $-f^2 H^2 \sigma^2$, while the present framework identifies an additional higher-order contribution proportional to σ^4 , consistent with a one-loop interpretation in perturbation theory.

The characteristic density parameter Ω_c is determined from a physically motivated identification of the epoch of peak stiffness with the peak halo formation rate at $z_{\text{halo}} = 1.1$ (Fakhouri, Ma & Boylan-Kolchin 2010), yielding

$$\Omega_c = 9.261 \Omega_m$$

This reduces the model to three free cosmological parameters (ω_m, H_0, σ_8), matching the parameter count of spatially flat Λ CDM.

Confrontation with Pantheon+ Type Ia supernovae (1580 SNe with full statistical and systematic covariance), BOSS DR12 BAO and growth-rate measurements, DESI DR1 BAO (7 bins spanning $z = 0.3$ – 2.3), and the model-independent Planck acoustic scale $\theta_* = 0.010409 \pm 0.000006$ evaluated self-consistently within EEC geometry yields:

$$\begin{aligned} H_0 &= 70.77 \pm 0.31 \text{ km s}^{-1} \text{ Mpc}^{-1} \\ S_8 &= \sigma_8 \sqrt{(\Omega_m/0.3)} = 0.754 \pm 0.036 \\ \Omega_m &= 0.3189 \pm 0.0045, \Omega_{\text{neq}} = 0.6810 \pm 0.0045 \end{aligned}$$

The predicted value of S_8 lies within 0.2σ of current weak-lensing survey constraints, while the inferred Hubble constant falls between the Planck and SH0ES determinations.

The best-fit statistic is

$$\chi^2 = 1441.4$$

for three free parameters, corresponding to

$$\chi^2/\text{dof} = 0.903,$$

compared with approximately $\chi^2 \approx 1410$ for Λ CDM. The resulting difference,

$$\Delta\chi^2 \approx 32$$

quantifies the EEC prediction of a time-varying equation of state.

The predicted CMB acoustic scale, $\theta_{*,\text{EEC}} = 0.010411$ is consistent with the Planck measurement, $\theta_* = 0.010409 \pm 0.000006$ at the level of $+0.27\sigma$. This resolves the 5.4σ tension present in v6, which arose from the use of the Λ CDM-geometry-dependent ω_m prior that is inconsistent with the EEC expansion history.

Keywords: cosmic acceleration; Emergent Dark Energy; Buchert backreaction; non-equilibrium thermodynamics; internal variables; nonlocal effective cosmology; structure formation; Pantheon+, BOSS DR12, DESI DR1; equation of state.

1. Introduction

The accelerating expansion of the universe, first established through observations of distant Type Ia supernovae and subsequently supported by measurements of the cosmic microwave background (CMB) and baryon acoustic oscillations (BAO), represents one of the central empirical discoveries of modern cosmology. Within the standard Λ CDM framework, this acceleration is attributed to a cosmological constant, Λ , whose associated energy density constitutes the dominant fraction of the present critical density.

Despite its observational success, this description raises two well-known theoretical challenges. The first is the vacuum energy problem, wherein the observed value of Λ is smaller than typical quantum field theory estimates by many orders of magnitude. The second is the coincidence problem, namely why the energy densities of matter and dark energy are of comparable magnitude precisely during the present cosmological epoch. These issues continue to motivate investigation into alternative explanations of cosmic acceleration that remain consistent with established observations.

One such direction is provided by the backreaction programme initiated by Buchert, which examines whether spatial averaging of the inhomogeneous Einstein equations can generate an effective acceleration term. In this framework, the non-commutativity of spatial averaging and the construction of the Einstein tensor gives rise to an additional contribution known as the kinematic backreaction,

$$Q_D$$

While the Buchert equations are exact within general relativity, a central unresolved issue has been the absence of a physically motivated closure relation connecting the backreaction term to observable statistical properties of the matter distribution.

The Emergent Expansion Cosmology (EEC) framework proposed in the present work aims to address this gap by providing a thermodynamically motivated closure for the Buchert equations. The central hypothesis is that the kinematic backreaction Q_D is related to the variance of matter density fluctuations evaluated at a characteristic nonlinear scale R_s , and that this contribution may be modeled as proportional to the square of that variance, with a coefficient informed by the Press–Schechter description of gravitational collapse. This establishes a connection between large-scale expansion dynamics and the statistical properties of cosmic structure formation.

At present, a complete derivation of this relation directly from general relativity—such as through a one-loop standard perturbation theory (SPT) calculation—remains an important open theoretical task. The present work therefore adopts a systematically constructed thermodynamic approach, with the goal of identifying a consistent and physically grounded closure relation that can be confronted with observational data.

The structure of this paper is as follows. Section 2 defines the scientific scope of the framework. Sections 3 and 4 describe the primordial high-density state and the activation of expansion. Sections 5 and 5a develop the thermodynamic formulation and the non-equilibrium free-energy sector. Sections 6 and 7 introduce the free-energy contribution and

the modified Friedmann equations. Subsequent sections establish the variational structure, demonstrate consistency with the second law of thermodynamics, and connect the framework to the Buchert formalism. The Bianchi identity is then verified explicitly, and the resulting cosmological dynamics are analyzed through the effective equation of state and expansion history. Linear perturbation theory, stability considerations, and the cosmic age are subsequently examined. The model is then confronted with observations, followed by a discussion of the energy budget and its physical interpretation. The final sections summarize the results, outline open problems, and present the principal conclusions.

2. Scientific Scope and Motivation

The Emergent Expansion Cosmology (EEC) framework is formulated as a nonlocal effective theory applicable on scales

$$R \gtrsim R_s$$

for which the matter distribution has entered the nonlinear regime and coarse-graining over inhomogeneities becomes necessary. On such scales, the governing equations are interpreted as spatially averaged quantities in the Buchert sense, rather than as strictly local relations.

For an irrotational dust cosmology, the Buchert equations provide an exact description of the averaged dynamics within general relativity:

$$3 \frac{\ddot{a}_D}{a_D} = -4\pi G \langle \rho \rangle_D + Q_D \quad (\text{B1})$$

$$3H_D^2 = 8\pi G \langle \rho \rangle_D - \frac{1}{2} Q_D - \frac{1}{2} \langle {}^3R \rangle_D \quad (\text{B2})$$

where a_D is the domain-dependent scale factor, H_D is the corresponding Hubble parameter, and angle brackets denote spatial averaging over a domain D .

The kinematic backreaction term is defined as

$$Q_D = \frac{2}{3} (\langle \theta^2 \rangle_D - \langle \theta \rangle_D^2) - 2 \langle \sigma_{\text{shear}}^2 \rangle_D$$

and encodes the variance of local expansion together with the contribution of shear within the averaging domain.

Although these equations are exact, they are not closed, since the evolution of Q_D and the averaged spatial curvature $\langle {}^3R \rangle_D$ is not determined solely by the averaged matter density. A physically motivated closure relation is therefore required in order to connect the backreaction sector to observable statistical properties of the cosmic matter distribution.

The EEC framework proposes such a closure by associating the kinematic backreaction with a thermodynamically defined non-equilibrium free energy of the coarse-grained matter distribution. In this interpretation, the backreaction term is not introduced phenomenologically, but instead emerges from the statistical properties of structure formation and from the redistribution of energy during gravitational collapse.

A key consistency requirement of this approach is that the characteristic scale and normalization of the non-equilibrium free energy admit a coherent description across the range of physical scales relevant to both structure formation and large-scale expansion. In particular, the framework links quantities defined on nonlinear clustering scales with those governing homogeneous background evolution, thereby providing a bridge between small-scale statistical physics and cosmic-scale dynamics.

This cross-scale consistency suggests that the proposed thermodynamic description captures a physically meaningful aspect of the underlying gravitational dynamics. Nevertheless, the present framework remains an effective theory, and further theoretical work is required to derive the closure relation directly from first principles within general relativity.

If cosmic acceleration is indeed driven by a thermodynamic free-energy contribution associated with structure formation, rather than by a fundamental vacuum-energy component, then the large discrepancy between quantum field theory estimates of vacuum energy and the observed value of Λ may not be directly relevant to the origin of acceleration within this framework.

3. The Primordial High-Density State

Prior to the formation of large-scale structure, the universe was highly homogeneous, with density fluctuations at the level of approximately one part in 10^5 . In this regime, the internal variable

$$\xi = \sigma^2(R_s, t)$$

which characterizes the variance of density fluctuations at the coarse-graining scale R_s , is correspondingly very small:

$$\xi \approx 0$$

Within the EEC framework, the effective stiffness function governing the non-equilibrium sector is modeled as

$$\kappa(\rho_m) \propto \left(\frac{\rho_m}{\rho_c}\right) e^{-\rho_m/\rho_c}$$

This functional form introduces a strong density-dependent suppression at high matter density. In particular, in the regime

$$\rho_m \gg \rho_c$$

the exponential factor ensures that the effective contribution to the dynamics becomes negligibly small.

As a consequence, the non-equilibrium free energy associated with structure formation is strongly suppressed in the early universe. Since the internal variable ξ is also vanishingly small in this regime, the combined effect yields an effectively negligible contribution of the EEC sector to the homogeneous background evolution.

Therefore, the standard early-universe sequence—including radiation domination, recombination, and formation of the cosmic microwave background—is preserved without modification at the background level within the present framework.

This self-limiting behavior is not imposed ad hoc, but instead arises as a structural consequence of the density-dependent stiffness function. The exponential dependence on matter density reflects the suppression of structure-formation processes in the high-density regime, where gravitational collapse has not yet generated significant nonlinear inhomogeneities.

Accordingly, the EEC contribution becomes dynamically relevant only at later epochs, when the matter density has sufficiently decreased and structure formation proceeds efficiently.

4. Activation of Expansion and Cosmic Dilution

As the universe expands, the mean matter density evolves according to

$$\rho_m(z) = \rho_{m0}(1+z)^3$$

leading to a continuous dilution of matter with cosmic time. Simultaneously, gravitational instability amplifies primordial density perturbations, driving the growth of large-scale structure through nonlinear collapse and clustering.

Within the EEC framework, the emergence of a significant non-equilibrium contribution is controlled by the relation between the matter density ρ_m and the characteristic density scale ρ_c . A natural reference epoch is defined by the condition

$$\rho_m(z_c) = \rho_c$$

which determines the transition redshift at which the density-dependent suppression becomes inefficient.

Using the standard matter-density evolution, this condition gives

$$(1+z_c)^3 = \frac{\rho_c}{\rho_{m0}}$$

or equivalently,

$$(1+z_c)^3 = \frac{\Omega_c}{\Omega_{m0}}$$

where Ω_c and Ω_{m0} denote the density parameters associated with ρ_c and the present-day matter density, respectively.

This transition epoch corresponds to the period during which structure formation becomes dynamically efficient and the suppression of the non-equilibrium sector is substantially reduced.

At redshifts

$$z \gtrsim z_c$$

the matter density remains sufficiently high that the exponential suppression factor limits the impact of the EEC contribution. As cosmic evolution proceeds toward lower redshift, ρ_m decreases and the suppression weakens, allowing the non-equilibrium free-energy term to become dynamically relevant.

At late times, when

$$\rho_m < \rho_c$$

the system evolves beyond the regime in which the effective contribution is maximized. Consequently, the EEC term is expected to decline gradually with time. This behavior contrasts with the standard Λ CDM model, in which the cosmological constant remains strictly constant.

This time dependence leads to potentially observable departures from the standard cosmological scenario. In particular, the framework predicts a redshift-dependent effective equation of state $w(z)$, together with modifications to the growth rate of structure, commonly expressed through observables such as

$$f\sigma_8(z)$$

These signatures provide a direct basis for empirical tests of the framework.

5. The Non-Equilibrium State and the Internal Variable ξ

5.1 The Universe as a Non-Equilibrium Thermodynamic System

The theoretical framework adopted in this work is based on the Coleman–Gurtin (1967) formulation of thermodynamics with internal state variables. This formalism provides a consistent description of systems out of thermodynamic equilibrium by introducing additional variables that encode internal structural evolution.

Within the EEC framework, this approach serves two primary purposes. First, it enables a systematic construction of the non-equilibrium free energy associated with structure formation. Second, it provides a basis for analyzing thermodynamic stability and consistency with the second law.

The internal variable ξ is identified with the variance of matter density fluctuations at a coarse-graining scale R_s :

$$\xi = \sigma^2(R_s, t)$$

Its evolution is determined by gravitational dynamics. In the linear regime of structure formation, the matter density contrast grows proportionally to the linear growth factor $D(z)$, such that

$$\delta_m(x, z) \propto D(z)$$

Consequently, the variance evolves as

$$\xi(z) = \sigma^2(R_s, z) \propto D^2(z)$$

and therefore the free-energy density, which is quadratic in ξ , scales as

$$f_{\text{neq}} \propto \xi^2 \propto D^4(z)$$

Normalizing to the present epoch gives

$$\xi^2(z) = \sigma_8^4 \frac{D^4(z)}{D^4(0)}$$

where σ_8 denotes the present-day root-mean-square variance at the scale R_s . This relation provides a direct connection between the non-equilibrium free energy and the growth of structure, without introducing additional free functions.

5.2 Mathematical Definition of the Local Internal Variable

The internal variable ξ is defined as the smoothed variance of the matter density contrast over a characteristic scale R_s . At the local level, this corresponds to a top-hat average of the squared density contrast:

$$\xi(x, t) = \frac{1}{V_s} \int_{|x'-x| \leq R_s} \delta_m^2(x', t) d^3x'$$

where

$$V_s = \frac{4}{3} \pi R_s^3$$

is the smoothing volume.

The quantity entering the background cosmological equations is the spatial average over a sufficiently large domain, which reduces to the variance of the matter power spectrum:

$$\xi(t) = \sigma^2(R_s, t) = \frac{1}{2\pi^2} \int_0^\infty P(k, t) W^2(kR_s) k^2 dk$$

where $P(k, t)$ is the matter power spectrum and $W(kR_s)$ is the smoothing window function.

For a top-hat filter at scale R_s , this expression corresponds to the standard definition of the variance of density fluctuations. In particular, choosing R_s to coincide with the conventional normalization scale yields

$$\xi(0) = \sigma_8^2$$

and therefore

$$\xi^2(0) = \sigma_8^4$$

thereby establishing a direct connection between the non-equilibrium free energy and observationally constrained quantities.

5.3 Timescale Separation and the Slow-Mode Identification

The internal variable

$$\xi = \sigma^2(R_s, t)$$

represents a coarse-grained quantity that averages over fast dynamical processes, such as virialized motions within gravitationally bound structures. These processes occur on characteristic timescales

$$t_{\text{dyn}} \ll H^{-1}$$

and therefore do not directly influence the large-scale expansion dynamics.

Instead, ξ captures the slow secular evolution associated with the growth of cosmic structure. Using the relation

$$\xi \propto D^2$$

one obtains

$$\frac{\dot{\xi}}{\xi} = 2 \frac{\dot{D}}{D}$$

Since the growth rate satisfies

$$\frac{\dot{D}}{D} \sim H$$

on cosmological scales, it follows that

$$\frac{\dot{\xi}}{\xi} \sim H$$

thereby justifying the treatment of ξ as a slowly varying background variable.

At linear order in perturbation theory, the relation

$$\xi^2(z) = \sigma_8^4 \frac{D^4(z)}{D^4(0)}$$

is exact, providing a well-defined and observationally grounded description of the evolution of the non-equilibrium free energy.

5.4 Effective Theory Status and Nonlocality

The EEC framework is formulated as a nonlocal effective theory. The stress-energy contribution associated with the non-equilibrium component depends on a spatial average over a finite region of characteristic size R_s , which is significantly smaller than the Hubble horizon scale.

This spatial averaging does not imply any violation of causality or superluminal signaling. Rather, it reflects the coarse-grained nature of the description, in which small-scale inhomogeneities are encoded into effective large-scale quantities.

The effective energy density

$$\rho_{\text{neq}} = f_{\text{neq}}$$

should therefore be interpreted as a Buchert-level coarse-grained quantity, rather than as a locally defined energy density in general relativity.

Since gravitational energy is not locally well-defined in general relativity, such effective descriptions are necessarily model-dependent and are appropriate only at the averaged level on which the EEC framework operates. This interpretation remains consistent with the action-based formulation at the homogeneous background level.

5a. Physical Motivation for the Non-Equilibrium Free Energy

5a.1 Quadratic Dependence on the Internal Variable

The non-equilibrium free energy is constructed as a function of the internal variable ξ , which represents the variance of density fluctuations. Since ξ is quadratic in the density contrast, and the underlying statistical distribution is symmetric under

$$\delta \rightarrow -\delta$$

the free energy must be an even function of ξ .

Expanding around the equilibrium state, the leading-order contribution therefore takes the form

$$f_{\text{neq}} \propto \xi^2$$

with a positive coefficient required to ensure thermodynamic stability.

For a Gaussian density field, this quadratic dependence is exact. Deviations from Gaussianity introduce higher-order corrections, beginning at cubic order in the fluctuation amplitude. These corrections generate subleading contributions to the effective coefficient and do not alter the leading-order structure of the free energy.

5a.2 Stiffness Function: Physical Motivation and Adopted Ansatz

The statistical properties of gravitational collapse may be described using the Press–Schechter formalism, in which the collapsed fraction of matter is given by

$$F_{\text{coll}} = \text{erfc} \left(\frac{\delta_c}{\sqrt{2} \sigma(R_s)} \right)$$

where δ_c is the critical collapse threshold.

The sensitivity of collapse processes to changes in the matter distribution can be characterized by the response of this collapsed fraction to variations in the background density. At leading order, this dependence may be expressed through derivatives of F_{coll} with respect to the variance σ , together with the dependence of σ on cosmological evolution.

Using the relation

$$\sigma^2 \propto D^2(z)$$

and the dependence of the growth factor on matter density, one obtains an effective density-dependent response function. This response captures the efficiency with which structure formation contributes to the non-equilibrium sector.

Motivated by the qualitative behavior of this response—which vanishes in both the low- and high-density limits and exhibits a single maximum—and by the Coleman–Gurtin admissibility requirements

$$\kappa \geq 0$$

with

$$\kappa \rightarrow 0 \text{ as } \rho_m \rightarrow 0$$

and

$$\kappa \rightarrow 0 \text{ as } \rho_m \rightarrow \infty$$

we adopt the ansatz

$$\kappa(\rho_m) = \kappa_0 \left(\frac{\rho_m}{\rho_c} \right) e^{-\rho_m/\rho_c}$$

This functional form satisfies the required limiting behavior and exhibits a maximum at

$$\rho_m = \rho_c$$

Its precise equivalence to the Press–Schechter response function has not been established rigorously, and this connection remains an open theoretical problem.

The characteristic density scale is defined by

$$\rho_c = \Omega_c \rho_{\text{crit},0}$$

thereby introducing a single additional parameter into the framework.

5a.3 Normalization and Consistency Across Scales

The normalization of the stiffness function is determined by the requirement that the non-equilibrium free energy provide a consistent description across the range of physical scales relevant to both structure formation and large-scale cosmological dynamics.

In particular, the framework relates quantities defined on nonlinear clustering scales to those governing the homogeneous background expansion. This connection yields a nontrivial consistency condition linking small-scale power-spectrum statistics with large-scale observables.

The resulting normalization constant κ_0 is not treated as an independent free parameter. Instead, it is fixed by consistency with the background cosmological dynamics, specifically through the normalization condition imposed on the expansion history.

In practice, this relates κ_0 to the parameters Ω_c, Ω_{m0}

and the normalization of the matter power spectrum, thereby determining its value once these quantities are specified.

As a result, the EEC framework introduces only a single additional free parameter beyond the standard cosmological model, namely the characteristic density parameter Ω_c .

6. The Non-Equilibrium Free Energy

The central quantity in the EEC framework is the non-equilibrium free-energy density, modeled as a function of the matter density ρ_m and the internal variable ξ .

In the vicinity of thermodynamic equilibrium, the free energy may be expanded as a function of the internal variable. Since the equilibrium state corresponds to

$$\xi = 0$$

and the system is symmetric under fluctuations of the underlying density field, the leading contribution takes the quadratic form

$$f_{\text{neq}}(\rho_m, \xi) = \frac{1}{2} \kappa(\rho_m) \xi^2$$

where the coefficient

$$\kappa(\rho_m) = \frac{\partial^2 f_{\text{neq}}}{\partial \xi^2}$$

acts as an effective stiffness function governing the response of the system to fluctuations.

Using the density-dependent stiffness function introduced in Section 5a.2, this becomes

$$f_{\text{neq}}(\rho_m, \xi) = \frac{\kappa_0}{2} \left(\frac{\rho_m}{\rho_c} \right) e^{-\rho_m/\rho_c} \xi^2$$

Since,

$$\xi = \sigma^2(R_s, t)$$

and the free energy is quadratic in ξ , the non-equilibrium contribution scales as the fourth power of the fluctuation amplitude:

$$f_{\text{neq}} \propto \xi^2 \propto \sigma^4 \propto D^4(z)$$

This behavior is consistent with a one-loop interpretation in perturbation theory.

By construction, the stiffness satisfies

$$\kappa(\rho_m) \geq 0$$

which ensures that the free energy is a convex function of the internal variable. Together with the normalization condition

$$f_{\text{neq}}(\xi = 0) = 0$$

this guarantees that $f_{\text{neq}} \geq 0$ as required for thermodynamic stability.

The functional form of $\kappa(\rho_m)$ further ensures that the non-equilibrium contribution vanishes in both the low-density and high-density limits, consistent with the suppression of structure formation in these regimes.

The normalization constant κ_0 is not treated as an independent free parameter. Instead, it is fixed by consistency with the homogeneous background cosmological dynamics, specifically through the normalization condition imposed on the expansion history.

In practice, this relates κ_0 to the parameters Ω_c, Ω_{m0} together with the normalization of the matter power spectrum, thereby determining its value once these quantities are specified.

7. Modified Friedmann Equations

7.1 Derivation of the Non-Equilibrium Pressure

The total internal energy density of the system is written as the sum of equilibrium and non-equilibrium contributions:

$$u(\rho_m, s, \xi) = u_{\text{eq}} + f_{\text{neq}}$$

where s denotes the entropy density and f_{neq} is the non-equilibrium free energy defined previously.

The corresponding non-equilibrium pressure is obtained from the thermodynamic identity for a relativistic fluid:

$$p_{\text{neq}} = \rho_m^2 \frac{d}{d\rho_m} \left(\frac{f_{\text{neq}}}{\rho_m} \right)_{\xi \text{ fixed}}$$

Substituting the expression for f_{neq} and evaluating the derivative at fixed ξ :

$$\frac{f_{\text{neq}}}{\rho_m} = \frac{\kappa_0}{2} \left(\frac{1}{\rho_c} \right) e^{-\rho_m/\rho_c} \xi^2$$

Taking the derivative with respect to ρ_m :

$$\frac{d}{d\rho_m} \left(\frac{f_{\text{neq}}}{\rho_m} \right) = -\frac{1}{\rho_c} \left(\frac{f_{\text{neq}}}{\rho_m} \right)$$

where the derivative acts only on the exponential factor. Multiplying by ρ_m^2 , one obtains

$$\boxed{p_{\text{neq}} = -\left(\frac{\rho_m}{\rho_c} \right) \rho_{\text{neq}}}$$

Where $\rho_{\text{neq}} = f_{\text{neq}}$

This establishes a direct relation between the non-equilibrium pressure and energy density, with a density-dependent effective equation of state.

7.2 The Complete Modified Friedmann Equations

Including the non-equilibrium contribution, the Friedmann equations take the form

$$H^2 = \frac{8\pi G}{3} (\rho_m + \rho_r + \rho_{\text{neq}})$$

$$\frac{\ddot{a}}{a} = -\frac{4\pi G}{3} (\rho_m + \rho_r + 3p_r) + \Gamma(\rho_m, \xi)$$

where p_r is the radiation pressure and $\Gamma(\rho_m, \xi)$ represents the emergent acceleration term arising from the non-equilibrium component.

This contribution follows from the combination

$$-\frac{4\pi G}{3}(\rho_{\text{neq}} + 3p_{\text{neq}})$$

Substituting the pressure relation gives

$$\rho_{\text{neq}} + 3p_{\text{neq}} = \rho_{\text{neq}} \left(1 - \frac{3\rho_m}{\rho_c}\right)$$

Substituting the explicit expression for ρ_{neq} , one obtains

$$\Gamma(\rho_m, \xi) = \frac{2\pi G \kappa_0}{3} \left(\frac{\rho_m}{\rho_c}\right) \left(\frac{3\rho_m}{\rho_c} - 1\right) e^{-\rho_m/\rho_c \xi^2}$$

This expression makes explicit how the sign and magnitude of the emergent contribution depend on both the matter density and the level of structure formation encoded in ξ .

7.3 Energy Conservation and the Source Term

The time derivative of

$$\rho_{\text{neq}} = f_{\text{neq}}(\rho_m, \xi)$$

receives contributions from both changing ξ and changing ρ_m :

$$\frac{d\rho_{\text{neq}}}{dt} = \left(\frac{\partial f_{\text{neq}}}{\partial \xi}\right) \dot{\xi} + \left(\frac{\partial f_{\text{neq}}}{\partial \rho_m}\right) \dot{\rho}_m$$

Using

$$\frac{\partial f_{\text{neq}}}{\partial \xi} = \kappa(\rho_m) \xi$$

the first term gives

$$Q = \kappa(\rho_m) \xi \dot{\xi}$$

When matter follows standard cold-dark-matter dilution,

$$\dot{\rho}_m + 3H\rho_m = 0$$

the second term evaluates to

$$-3H(\rho_{\text{neq}} + p_{\text{neq}})$$

yielding the non-equilibrium continuity equation:

$$\boxed{\dot{\rho}_{\text{neq}} + 3H(\rho_{\text{neq}} + p_{\text{neq}}) = \kappa(\rho_m) \xi \dot{\xi}}$$

The right-hand side represents the rate at which gravitational potential energy—released during structure formation and encoded in the growth of ξ —is converted into non-equilibrium free energy. In the Buchert interpretation, this energy is drawn from the nonlocal gravitational sector rather than from the cold-dark-matter rest-mass density.

Accordingly, the matter continuity equation remains unmodified:

$$\dot{\rho}_m + 3H\rho_m = 0$$

and therefore $\rho_m \propto (1+z)^3$ exactly.

Importantly, the source terms cancel identically when the continuity equations are combined, ensuring that the total energy-momentum tensor remains conserved. This guarantees consistency with the covariant conservation laws of general relativity at the homogeneous background level.

Correction to earlier draft: A previous version of this section wrote the matter equation as $\dot{\rho}_m + 3H\rho_m = -Q$ and stated that $Q \ll 3H\rho_m$. This formulation is internally inconsistent. If $\rho_m \propto (1+z)^3$, then $\dot{\rho}_m + 3H\rho_m = 0$ exactly, implying $Q = 0$, which contradicts $Q = \kappa\dot{\xi}\dot{\xi} \neq 0$. The correct interpretation is the one adopted here: Q represents energy drawn from the gravitational-potential sector in the Buchert sense, not a drain on cold-dark-matter rest mass.

7.4 Variational Formulation, Sound Speed, and the Second Law

7.4.1 The Action Principle and the Pressure

The non-equilibrium sector may be formulated at the level of an action:

$$S_{\text{neq}} = \int d^4x \sqrt{-g} \mathcal{L}_{\text{neq}}$$

with Lagrangian density

$$\mathcal{L}_{\text{neq}} = -f_{\text{neq}}(\rho_m, \xi)$$

This choice follows from the standard result for relativistic perfect fluids that the matter Lagrangian in the local rest frame is given by $-\rho$. In the present framework, the internal variable ξ is treated as a coarse-grained quantity and is therefore held fixed under variation.

Performing the Hilbert variation of the action with respect to the metric, at fixed ξ , yields the stress-energy tensor

$$T_{\mu\nu}^{\text{neq}} = -\frac{2}{\sqrt{-g}} \frac{\delta S_{\text{neq}}}{\delta g^{\mu\nu}}$$

Since the Lagrangian depends on the metric only through the density ρ_m , the variation induces

$$\delta f_{\text{neq}} = \left(\frac{\partial f_{\text{neq}}}{\partial \rho_m} \right) \delta \rho_m$$

Using the standard relation for relativistic fluids,

$$\delta \rho_m = \frac{1}{2} (\rho_m + p_m) g_{\mu\nu} \delta g^{\mu\nu}$$

one recovers a perfect-fluid form of the stress-energy tensor, with effective pressure

$$p_{\text{neq}} = \rho_m^2 \frac{d}{d\rho_m} \left(\frac{f_{\text{neq}}}{\rho_m} \right)_{\xi}$$

This reproduces exactly the pressure derived previously, establishing that the pressure assignment is consistent with the variational principle within the adopted Lagrangian prescription.

7.4.2 Sound Speed and Perturbative Stability

The effective sound speed associated with the non-equilibrium component is

$$c_s^2 = \left(\frac{dp_{\text{neq}}}{d\rho_{\text{neq}}} \right)_{\rho_m, \xi} = -\frac{\rho_m}{\rho_c} < 0$$

In a conventional fluid, a negative sound-speed squared would indicate a Jeans-type instability. However, the present system differs in an important respect. At linear order in perturbation theory, one finds

$$\delta\xi = 0$$

(see Section 18.1), so that perturbations in ρ_{neq} are not independent propagating degrees of freedom, but are instead sourced by perturbations in the matter density $\delta\rho_m$.

As a result, the non-equilibrium component does not support freely propagating modes. The negative sound speed modifies the response of the system — encoded through the effective coupling $\mu(z)$ — but does not generate independent growing instabilities.

Within this approximation, the framework remains perturbatively stable at linear order. Nonlinear stability has not yet been examined.

7.4.3 Entropy Production and the Second Law during Active Structure Formation

The entropy production associated with the non-equilibrium component may be written as

$$\dot{S}_{\text{neq}} = \frac{Q}{T_{\text{eff}}} = \frac{\kappa(\rho_m)\xi\dot{\xi}}{T_{\text{eff}}}$$

The non-negativity of this expression follows directly from the properties of the constituent quantities:

$$\kappa(\rho_m) \geq 0, \xi = \sigma^2 \geq 0, T_{\text{eff}} > 0$$

together with the condition

$$\dot{\xi} \geq 0$$

during epochs of active structure formation.

The second law of thermodynamics is therefore satisfied as a structural consequence of the dynamics during the epoch of active structure formation, rather than being imposed as an external assumption.

The condition $\dot{\xi} \geq 0$ holds throughout the matter-dominated and accelerating eras, though it need not hold in all possible regimes. Accordingly, the second law is satisfied throughout the cosmologically relevant epoch considered here, providing an important internal consistency check on the framework.

7.5 Connection to the Buchert Equations and the One-Loop Context

7.5.1 The EEC Closure Relation

Comparing the modified acceleration equation with the Buchert acceleration equation, one obtains the effective closure relation

$$Q_D \sim \frac{2\pi G \kappa_0}{3} \left(\frac{\rho_m}{\rho_c} \right) \left(\frac{3\rho_m}{\rho_c} - 1 \right) e^{-\rho_m/\rho_c} \sigma^4(R_s, t)$$

This expression provides a physically motivated mapping between the kinematic backreaction term and the statistical properties of the matter distribution.

7.5.2 The One-Loop Perturbation Theory Context

At linear order, using the continuity relation

$$\theta_k = -fH\delta_k$$

the Buchert backreaction reduces to

$$Q_D^{\text{linear}} = -\frac{2}{3} f^2 H^2 \sigma^2(R_s) < 0$$

indicating that the leading-order contribution is negative and therefore contributes to deceleration. This is the standard result within the Buchert framework.

The EEC contribution does not appear at linear order and is therefore subleading in this regime. At second order (one-loop level), the velocity-divergence power spectrum acquires corrections of the schematic form

$$Q_D^{(1\text{-loop})} \sim A_1(z) f^2 H^2 \sigma^2(R_s) + A_2(z) \sigma^4(R_s) + O(\sigma^6)$$

Within this structure, the EEC closure identifies the dominant accelerating contribution with the σ^4 term, such that

$$A_2(z) \leftrightarrow \frac{2\pi G \kappa_0}{3} \left(\frac{\rho_m}{\rho_c} \right) \left(\frac{3\rho_m}{\rho_c} - 1 \right) e^{-\rho_m/\rho_c}$$

This identification should be interpreted as a physically motivated ansatz rather than as a formally derived result.

A complete verification requires an explicit computation of $A_2(z)$ from one-loop standard perturbation theory or from numerical N -body simulations, followed by comparison with the functional form implied by the Press–Schechter-motivated stiffness function.

This remains the principal outstanding theoretical task of the framework.

8. Bianchi Consistency Verification

A necessary consistency condition for any modification of the Friedmann equations is compatibility with the Bianchi identity, which ensures the covariant conservation of the total energy–momentum tensor in general relativity.

To verify this explicitly, we differentiate the modified Friedmann equation

$$H^2 = \frac{8\pi G}{3}(\rho_m + \rho_r + \rho_{\text{neq}})$$

with respect to time and obtain

$$2H\dot{H} = \frac{8\pi G}{3}(\dot{\rho}_m + \dot{\rho}_r + \dot{\rho}_{\text{neq}}).$$

Substituting the continuity equations for matter,

$$\dot{\rho}_m + 3H\rho_m = 0,$$

radiation,

$$\dot{\rho}_r + 4H\rho_r = 0$$

and the non-equilibrium component,

$$\dot{\rho}_{\text{neq}} + 3H(\rho_{\text{neq}} + p_{\text{neq}}) = Q$$

one finds that the source terms Q cancel exactly when the equations are combined. Explicitly,

$$\dot{\rho}_m + \dot{\rho}_{\text{neq}} = -3H\rho_m - 3H(\rho_{\text{neq}} + p_{\text{neq}})$$

so that

$$\dot{\rho}_{\text{tot}} = -3H(\rho_m + \rho_{\text{neq}} + p_{\text{neq}}) - 4H\rho_r$$

Substituting back and using

$$\frac{\ddot{a}}{a} = \dot{H} + H^2$$

together with the Friedmann equation, the resulting expression can be rearranged to yield

$$\frac{\ddot{a}}{a} = -\frac{4\pi G}{3}(\rho_m + \rho_r + 3p_r) - \frac{4\pi G}{3}(\rho_{\text{neq}} + 3p_{\text{neq}})$$

This reproduces the modified acceleration equation provided that

$$p_{\text{neq}} = -\left(\frac{\rho_m}{\rho_c}\right)\rho_{\text{neq}}$$

This demonstrates that the modified Friedmann system is internally consistent and respects the Bianchi identity at the background level.

Importantly, this result holds for any choice of the stiffness function $\kappa(\rho_m)$ and for any evolution of the internal variable $\xi(t)$, provided the coupled conservation equations are satisfied. The consistency therefore does not depend on the specific functional form of the closure, but follows from the structure of the framework itself.

9. Thermodynamic Foundation and Entropy Production

Within the EEC framework, the source term

$$Q = \kappa(\rho_m) \dot{\xi}$$

has a direct thermodynamic interpretation. It represents the irreversible conversion of gravitational potential energy, released during structure formation, into non-equilibrium free energy stored in the coarse-grained matter distribution.

This process is intrinsically dissipative at the effective level and is associated with entropy production. As established previously, the entropy production rate satisfies

$$\dot{S}_{\text{neq}} \geq 0$$

thereby ensuring consistency with the second law of thermodynamics during the epoch of active structure formation.

The evolution of entropy production is governed by the interplay between the stiffness function $\kappa(\rho_m)$ and the growth rate of structure $\dot{\xi}$. During the era of active structure formation, both quantities are non-negligible, leading naturally to a peak in entropy production at intermediate redshifts.

At later times, two effects suppress further entropy production.

First, the stiffness function decreases as the matter density declines:

$$\kappa(\rho_m) \rightarrow 0 \text{ as } \rho_m \rightarrow 0$$

reflecting the reduced efficiency of gravitational collapse in an increasingly dilute universe.

Second, the growth of structure slows and eventually saturates:

$$\dot{\xi} \rightarrow 0$$

as nonlinear bound structures become dynamically stable.

As a consequence, the entropy production rate asymptotically approaches zero in the far future:

$$\dot{S}_{\text{neq}} \rightarrow 0$$

indicating that the system evolves toward a state of effective thermodynamic equilibrium.

Within this framework, the long-term cosmological evolution differs qualitatively from that of the standard Λ CDM model. Rather than approaching an asymptotic de Sitter phase with constant expansion rate, the expansion in EEC gradually slows, with

$$H \rightarrow 0$$

at late times. This behavior reflects the exhaustion of the non-equilibrium free-energy source associated with structure formation.

10. The Effective Equation of State

10.1 The General Formula

The effective equation of state associated with the non-equilibrium component is defined as

$$w_{\text{neq}} = \frac{p_{\text{neq}}}{\rho_{\text{neq}}}$$

For the specific stiffness function introduced in this framework, the pressure–energy relation derived in Section 7 yields the exact expression

$$w_{\text{neq}} = -\frac{\rho_m}{\rho_c}$$

More generally, for an arbitrary stiffness function $\kappa(\rho_m)$, the equation of state can be written as

$$w_{\text{neq}} = -1 + \frac{d \ln \kappa}{d \ln \rho_m}$$

This relation follows directly from the general structure of the non-equilibrium free energy,

$$f_{\text{neq}} = \frac{1}{2} \kappa(\rho_m) \xi^2$$

together with the thermodynamic identity for the pressure. To make this explicit, one writes

$$\frac{f_{\text{neq}}}{\rho_m} = \frac{1}{2} \kappa(\rho_m) \xi^2 \left(\frac{1}{\rho_m} \right)$$

and differentiates with respect to ρ_m at fixed ξ . Applying the product rule gives

$$p_{\text{neq}} = \rho_m^2 \left[\frac{1}{2} \xi^2 \left(\frac{1}{\rho_m} \frac{d\kappa}{d\rho_m} - \frac{\kappa}{\rho_m^2} \right) \right] = \frac{1}{2} \xi^2 \left(\rho_m \frac{d\kappa}{d\rho_m} - \kappa \right)$$

Using

$$\rho_{\text{neq}} = f_{\text{neq}} = \frac{1}{2} \kappa \xi^2$$

the equation of state becomes

$$w_{\text{neq}} = \frac{\rho_m}{\kappa} \frac{d\kappa}{d\rho_m} - 1 = -1 + \frac{d \ln \kappa}{d \ln \rho_m}$$

This expression demonstrates that the equation of state is determined entirely by the logarithmic slope of the stiffness function, independently of the normalization of the free energy.

10.2 The Result $w = -1$ at the Characteristic Density

At the characteristic density

$$\rho_m = \rho_c$$

the stiffness function $\kappa(\rho_m)$ reaches its maximum. At this point,

$$\frac{d\kappa}{d\rho_m} = 0 \Rightarrow \frac{d \ln \kappa}{d \ln \rho_m} = 0$$

Substituting into the general expression yields

$$w_{\text{neq}}(\rho_m = \rho_c) = -1$$

This result holds for any admissible stiffness function that exhibits a maximum at the characteristic density, within the adopted pressure prescription. It does not depend on the specific functional form of $\kappa(\rho_m)$, but is conditional on the pressure formula introduced in Section 7.1.

10.3 The $w(z)$ Trajectory

For the specific parametrization adopted in this framework:

$$w(z) = -\left(\frac{\Omega_{m0}}{\Omega_c}\right)(1+z)^3$$

At the redshift defined by the condition

$$\rho_m = \rho_c$$

one has

$$w = -1$$

in agreement with the general result derived above.

At late times, when

$$\rho_m \ll \rho_c$$

the equation of state approaches

$$w \rightarrow 0$$

and the non-equilibrium component behaves effectively as pressureless matter.

This asymptotic behavior represents a key qualitative distinction from the standard cosmological model.

10.4 Total Effective Equation of State

The total effective equation of state of the cosmic fluid is given by

$$w_{\text{eff}}(z) = \frac{p_{\text{neq}}(z)}{\rho_m(z) + \rho_r(z) + \rho_{\text{neq}}(z)}$$

This quantity provides a direct characterization of the expansion dynamics of the universe within the EEC framework.

11. The Three Cosmic Evolution Regimes

11.1 Early Universe

At high redshift,

$$z \gg z_c$$

the stiffness function is exponentially suppressed:

$$\kappa(\rho_m) \propto e^{-\rho_m/\rho_c} \rightarrow 0$$

The non-equilibrium contribution is therefore effectively negligible, and the standard cosmological evolution is recovered at the background level, including radiation domination at early times and the subsequent matter-dominated era.

11.2 Intermediate Epoch: Active Acceleration

As the universe expands, the matter density decreases and approaches the characteristic scale,

$$\rho_m \sim \rho_c$$

The stiffness function reaches its maximum and the non-equilibrium contribution becomes dynamically significant.

The onset of accelerated expansion occurs when the non-equilibrium sector becomes sufficiently large to overcome the decelerating influence of matter, at a redshift that is generally distinct from z_c .

11.3 Late and Far Universe: Asymptotic Deceleration

At late times,

$$\rho_m \ll \rho_c$$

the stiffness vanishes:

$$\kappa \rightarrow 0$$

structure growth saturates:

$$\dot{\xi} \rightarrow 0$$

the non-equilibrium energy density diminishes:

$$\rho_{\text{neq}} \rightarrow 0$$

and the expansion rate decreases:

$$H \rightarrow 0$$

The universe therefore approaches a state of effective thermodynamic equilibrium.

This asymptotic behavior differs qualitatively from the de Sitter future of the Λ CDM model. It should be noted, however, that this long-term prediction follows from the specific structure of the present model and depends on the continued validity of the effective description at very late times.

12. Plateau Behaviour of the Effective Equation of State

In the vicinity of the characteristic density

$$\rho_m = \rho_c$$

the stiffness function reaches its maximum. At this point,

$$\frac{d\kappa}{d\rho_m} \approx 0$$

and

$$\frac{d^2\kappa}{d\rho_m^2}$$

is small, resulting in a relatively flat dependence of κ on ρ_m .

Through the general relation

$$w_{\text{neq}} = -1 + \frac{d\ln \kappa}{d\ln \rho_m}$$

this behavior translates into a plateau in the effective equation of state, with

$$w_{\text{neq}} \approx -1$$

over a finite interval in redshift.

Within this interval, the expansion history predicted by the EEC framework closely resembles that of the standard Λ CDM model, making the two scenarios observationally difficult to distinguish using background expansion data alone.

Discriminating signatures arise outside this plateau region. In particular, the model predicts:

- A deviation of the equation of state from $w = -1$ at redshifts above the characteristic scale, following the redshift-dependent trajectory determined by the density evolution.
- A modified growth rate of structure, encoded in the observable quantity

$$f\sigma_8(z)$$

through the redshift-dependent effective coupling $\mu(z)$.

- An exact vanishing of the gravitational slip parameter,

$$\eta = 0$$

where

$$\eta \equiv \Phi/\Psi - 1$$

which provides a distinctive prediction at the level of linear perturbations.

These features offer potential observational tests capable of distinguishing the EEC framework from the standard cosmological model, particularly when combined with measurements of both the expansion history and the growth of structure.

13. The Dimensionless Expansion Equation

13.1 The Coupled Self-Consistent System

The expansion history is expressed in terms of the dimensionless Hubble parameter

$$E(z) = \frac{H(z)}{H_0}$$

Within the EEC framework:

$$E^2(z) = \Omega_{m0}(1+z)^3 + \Omega_{r0}(1+z)^4 + \Omega_{\text{neq}}(z)$$

where

$$\Omega_{\text{neq}}(z) = \frac{\tilde{\kappa}_0}{2} \left(\frac{\Omega_{m0}}{\Omega_c} \right) (1+z)^3 e^{-(\Omega_{m0}/\Omega_c)(1+z)^3} \frac{D_{\text{EEC}}^4(z)}{D_{\text{EEC}}^4(0)}$$

The fourth-power dependence on the growth factor reflects the scaling

$$f_{\text{neq}} \propto \xi^2 \propto \sigma^4 \propto D^4$$

The equations for $E(z)$ and $\Omega_{\text{neq}}(z)$ form a coupled system, since the expansion rate influences the growth of structure, while the growth factor determines the magnitude of $\Omega_{\text{neq}}(z)$. This mutual dependence requires iterative solution.

13.2 The Normalization Condition

The normalization of the non-equilibrium contribution is fixed by the flatness condition at the present epoch. Since

$$\Omega_{\text{neq}}(0) = 1 - \Omega_{m0} - \Omega_{r0}$$

and

$$\xi^2(0) = \sigma_8^4$$

this leads to

$$\tilde{\kappa}_0 = \frac{2(1 - \Omega_{m0} - \Omega_{r0})}{(\Omega_{m0}/\Omega_c) e^{-\Omega_{m0}/\Omega_c} \sigma_8^4}$$

This expression determines $\tilde{\kappa}_0$ entirely in terms of Ω_c , Ω_{m0} , and σ_8 . Consequently, $\tilde{\kappa}_0$ is not an independent parameter.

The EEC framework therefore introduces only a single additional free parameter,

$$\Omega_c$$

beyond those of the standard cosmological model.

Note: The dimensionless normalization is denoted by $\tilde{\kappa}_0$, while κ_0 refers to its physical form.

13.3 Construction of the Dimensionless System

The non-equilibrium energy density is

$$\rho_{\text{neq}}(z) = \frac{\kappa_0}{2} \left(\frac{\Omega_{m0}}{\Omega_c} \right) (1+z)^3 e^{-(\Omega_{m0}/\Omega_c)(1+z)^3} \xi^2(z) \rho_{\text{crit},0}$$

Dividing by $\rho_{\text{crit},0}$ and substituting

$$\xi^2(z) = \sigma_8^4 \frac{D^4(z)}{D^4(0)}$$

gives

$$\Omega_{\text{neq}}(z) = \frac{\kappa_0}{2} \left(\frac{\Omega_{m0}}{\Omega_c} \right) (1+z)^3 e^{-(\Omega_{m0}/\Omega_c)(1+z)^3} \sigma_8^4 \frac{D^4(z)}{D^4(0)}$$

This makes explicit that the non-equilibrium contribution depends on the growth factor $D(z)$, forming the closed feedback loop:

$$E(z) \rightarrow D(z) \rightarrow \xi(z) \rightarrow \Omega_{\text{neq}}(z) \rightarrow E(z)$$

13a. Physically Motivated Determination of the Characteristic Density Scale

13a.1 The Role of ρ_c

The characteristic density ρ_c defines the epoch z_c at which the stiffness function $\kappa(\rho_m)$ reaches its maximum and the non-equilibrium equation of state satisfies

$$w_{\text{neq}} = -1$$

(see Section 10.2). Whether this scale can be predicted from the physics of structure formation, rather than treated as a free parameter, is addressed in the present section.

13a.2 Connection to the Halo Mass Function

The stiffness function $\kappa(\rho_m)$ is motivated by Press–Schechter collapse statistics (Section 5a.2). Its sensitivity to density changes is qualitatively consistent with the adopted ansatz

$$\left(\frac{\rho_m}{\rho_c} \right) e^{-\rho_m/\rho_c}$$

The peak of κ , and therefore the epoch z_c , corresponds to the period during which structure formation most efficiently converts gravitational energy into non-equilibrium free energy within the model.

13a.3 Peak Halo Formation Rate

For the coarse-graining scale

$$R_s = 8 h^{-1} \text{ Mpc}$$

the density variance $\sigma^2(R_s)$ is dominated by halos in the approximate mass range

$$M \sim 10^{12} - 10^{13} M_\odot$$

corresponding to Milky Way to galaxy-group scales.

Fakhouri, Ma & Boylan-Kolchin (2010, *MNRAS* 406, 2267) measured halo merger rates using the Millennium N -body simulations and found that the mean merger rate per halo peaks at

$$z_{\text{halo}} = 1.1$$

for halos in this mass range.

This epoch represents the maximum rate of gravitational collapse at the relevant scale.

13a.4 The Identification

Identifying

$$z_c = z_{\text{halo}}$$

implies

$$\rho_m(z_{\text{halo}}) = \rho_c$$

Using

$$\rho_m(z) = \rho_{m0}(1+z)^3$$

one obtains

$$\boxed{\Omega_c = \Omega_m(1+z_{\text{halo}})^3 = 9.261 \Omega_m}$$

Since

$$\Omega_m = \frac{\omega_m}{h^2}$$

the value of Ω_c varies self-consistently with the cosmological free parameters.

This identification is physically motivated, though it should be noted that the merger-rate peak reported by Fakhouri et al. occurs at somewhat different redshifts for different halo mass ranges, and the correspondence between the merger-rate peak and the stiffness-function peak remains an assumption rather than a rigorous derivation.

With this identification imposed, the model contains three free cosmological parameters:

$$(\omega_m, H_0, \sigma_8)$$

matching the parameter count of spatially flat Λ CDM.

13a.5 Consistency Checks

(i) Acceleration ordering

The acceleration transition satisfies $z_t < z_c$ consistent with the requirement that Ω_{neq} must accumulate before overcoming matter-driven deceleration (see Section 17).

(ii) Sound-horizon preservation

At

$$z_{\text{drag}} \sim 1019$$

one has

$$x = \frac{\Omega_m(1061)^3}{\Omega_c} \sim 10^8$$

so that

$$e^{-x} \approx 0$$

Hence, the EEC contribution is negligible near recombination, preserving standard CMB background physics.

(iii) Constructed coincidence

The derived value

$$z_c = 1.1$$

coincides with the epoch of peak halo merger rate by construction.

(iv) Falsifiability

Future measurements of the halo mass function from missions such as **Euclid** and the **Nancy Grace Roman Space Telescope** can independently constrain z_{halo} , thereby providing a direct observational test of this identification.

14. Self-Consistent Iteration and Convergence

The coupled system defined by the modified expansion equation, the non-equilibrium contribution, and the growth equation is solved through an iterative procedure, since $E(z)$ and $D_{\text{EEC}}(z)$ are mutually dependent.

The iteration proceeds as follows:

1. **Initial guess:**

The procedure is initialized using the Λ CDM growth factor as a starting approximation for $D(z)$.

2. **Update of $\Omega_{\text{neq}}(z)$:**

Using the current estimate of the growth factor, the non-equilibrium contribution is computed from its defining expression.

3. **Update of $E(z)$:**

The dimensionless expansion rate is obtained from the modified Friedmann equation.

4. **Growth-equation solution:**

The growth equation is solved using the updated expansion history, yielding a new estimate for the growth factor.

5. **Normalization:**

The growth factor is renormalized such that

$$D_{\text{EEC}}(0) = 1$$

6. **Convergence check:**

The iteration is repeated until successive updates of the growth factor differ by less than a prescribed tolerance (relative tolerance 10^{-6}) across the relevant redshift range.

The iterative scheme converges throughout the physically relevant parameter space, providing numerical evidence that the coupled system admits a stable and self-consistent solution.

The resulting functions

$$E(z), D_{\text{EEC}}(z)$$

are used for all subsequent predictions and analyses.

15. Predicted Expansion History

The EEC prediction for $E(z)$ exhibits small but systematic deviations from the standard cosmological model at intermediate and higher redshifts, while remaining very close to Λ CDM at low redshift.

This behavior reflects the plateau structure of the effective equation of state, which generates a near-degeneracy with the standard model over a finite redshift interval.

A key observable for testing the expansion history is the luminosity distance:

$$d_L(z) = (1 + z) \frac{c}{H_0} \int_0^z \frac{dz'}{E(z')}$$

Using the converged EEC solution for $E(z)$, this relation provides a description of distance–redshift observations consistent with current Type Ia supernova data.

16. The Deceleration Parameter

The deceleration parameter provides a direct measure of whether the cosmic expansion is accelerating or decelerating:

$$q(z) = -1 + \frac{1 + z}{2E^2(z)} \frac{dE^2(z)}{dz}$$

At the present epoch,

$$z = 0$$

the EEC framework predicts a negative value of the deceleration parameter, indicating accelerated expansion, in agreement with observations.

At higher redshift, deviations from the standard cosmological model become more pronounced and may be accessible to future observational surveys.

17. Transition from Deceleration to Acceleration

The transition from decelerating to accelerating expansion is defined by the condition

$$q(z_t) = 0$$

It is important to distinguish this transition redshift z_t from the characteristic redshift z_c , defined by the condition

$$\rho_m = \rho_c$$

at which the stiffness function reaches its maximum.

The onset of accelerated expansion is not determined solely by the requirement

$$w_{\text{neq}} < -\frac{1}{3}$$

but also requires that the non-equilibrium energy density become sufficiently large relative to the matter density.

This can be seen directly from the acceleration equation:

$$\frac{\ddot{a}}{a} = -\frac{4\pi G}{3}(\rho_m + \rho_r + 3p_r) - \frac{4\pi G}{3}(\rho_{\text{neq}} + 3p_{\text{neq}})$$

Neglecting radiation at late times, the condition for acceleration becomes

$$\rho_m + \rho_{\text{neq}} \left(1 - \frac{3\rho_m}{\rho_c}\right) < 0$$

or, in terms of density parameters,

$$\Omega_{\text{neq}} \left(\frac{3\rho_m}{\rho_c} - 1\right) > \Omega_m$$

This inequality is satisfied only after Ω_{neq} has grown to a sufficiently large value at redshifts below the characteristic scale.

The separation between z_t and z_c therefore constitutes a specific and testable prediction of the EEC framework.

17. Transition from Deceleration to Acceleration

The transition from decelerating to accelerating expansion is defined by the condition

$$q(z_t) = 0$$

which determines the transition redshift z_t .

It is important to distinguish this transition redshift from the characteristic redshift defined by the condition

$$\rho_m = \rho_c$$

at which the stiffness function reaches its maximum.

The condition for accelerated expansion is not determined solely by the equation of state satisfying

$$w_{\text{neq}} < -\frac{1}{3}$$

but also requires that the non-equilibrium energy density becomes sufficiently large relative to the matter density. In other words, acceleration depends on both the pressure and the fractional contribution of the non-equilibrium component.

This can be seen explicitly from the acceleration equation,

$$\frac{\ddot{a}}{a} = -\frac{4\pi G}{3}(\rho_m + \rho_r + 3p_r) - \frac{4\pi G}{3}(\rho_{\text{neq}} + 3p_{\text{neq}})$$

Neglecting radiation at late times, the condition for acceleration becomes

$$\rho_m + \rho_{\text{neq}} + 3p_{\text{neq}} < 0$$

Using the relation

$$p_{\text{neq}} = -\left(\frac{\rho_m}{\rho_c}\right)\rho_{\text{neq}}$$

these yields

$$\rho_m + \rho_{\text{neq}}\left(1 - \frac{3\rho_m}{\rho_c}\right) < 0$$

Dividing by the critical density and expressing in terms of density parameters, the exact condition for acceleration is

$$\Omega_{\text{neq}}\left(\frac{3\rho_m}{\rho_c} - 1\right) > \Omega_m$$

This condition is satisfied only after Ω_{neq} has grown to a sufficiently large value at redshifts below the characteristic scale.

This explains the offset between the transition redshift z_t and the characteristic redshift defined by $\rho_m = \rho_c$: while the equation of state reaches $w_{\text{neq}} = -1$ at the characteristic density, the energy density associated with the non-equilibrium component continues to grow for some time thereafter, delaying the onset of acceleration.

The separation between these two redshifts represents a specific and testable prediction of the EEC framework. In principle, it can be constrained observationally through a combination of distance measurements and growth rate data, which together probe both the expansion history and the relative contributions of different energy components.

18. Linear Perturbation Theory

18.1 Exact Vanishing of $\delta\xi$ at Linear Order

The internal variable

$$\xi = \sigma^2(R_s, t)$$

is defined as the spatial average of the squared matter density contrast:

$$\xi = \langle \delta_m^2 \rangle$$

Since ξ is quadratic in δ_m , its perturbation at first order is necessarily second order in the perturbation amplitude:

$$\delta_m = \delta_m^{(1)} + \delta_m^{(2)} + \dots$$

which implies

$$\xi = \langle (\delta_m^{(1)})^2 \rangle + \mathcal{O}(\delta_m^{(1)}\delta_m^{(2)})$$

Consequently,

$$\delta\xi^{(1)} = 0$$

exactly at linear order.

This result has important implications: the internal variable does not introduce an independent perturbation degree of freedom at linear order and therefore does not generate additional dynamical modes beyond those already present in the matter sector.

18.2 The Modified Poisson Equation

Given that $\delta\xi = 0$ at linear order, perturbations in the non-equilibrium energy density arise solely through their dependence on the matter density. Starting from

$$\rho_{\text{neq}} = f_{\text{neq}}(\rho_m, \xi)$$

and varying at fixed ξ , one obtains

$$\delta\rho_{\text{neq}} = \left(\frac{\partial f_{\text{neq}}}{\partial \rho_m} \right) \delta\rho_m$$

Using the explicit form of the free energy, this yields

$$\delta\rho_{\text{neq}} = \left(1 - \frac{\rho_m}{\rho_c} \right) \left(\frac{\rho_{\text{neq}}}{\rho_m} \right) \delta\rho_m$$

where the prefactor arises from the derivative of the density-dependent stiffness function.

Substituting into the Poisson equation leads to a modified relation,

$$-k^2\Phi = 4\pi G\rho_m \delta_m \mu(z)$$

where the effective gravitational coupling is given by

$$\mu(z) = 1 + \left(1 - \frac{\rho_m(z)}{\rho_c} \right) \frac{\Omega_{\text{neq}}(z)}{\Omega_m(z)}$$

At high redshift, where $\rho_m \gg \rho_c$ and $\Omega_{\text{neq}} \rightarrow 0$, one recovers

$$\mu(z) \rightarrow 1$$

corresponding to standard gravity.

At intermediate redshifts, where $\rho_m < \rho_c$, the correction term becomes positive,

$$\mu(z) > 1$$

leading to a mild enhancement of the effective gravitational coupling.

18.3 The Vanishing Slip Parameter

The non-equilibrium free energy f_{neq} depends only on scalar quantities and does not introduce anisotropic stress. As a result, the two scalar metric potentials remain equal:

$$\Phi = \Psi$$

The gravitational slip parameter is therefore

$$\eta = \frac{\Phi}{\Psi} - 1 = 0$$

This is an exact and parameter-independent prediction of the framework.

It provides a clear observational discriminator, since many modified-gravity models predict

$$\eta \neq 0$$

and future precision measurements may help distinguish between competing scenarios.

18.4 The EEC Growth Equation

The growth of linear matter perturbations is governed by the coupled system of the continuity, Euler, and Poisson equations in an expanding background.

For pressureless matter, the linearized continuity and Euler equations in Fourier space are given by

$$\begin{aligned}\delta_m + \frac{1}{a}\theta &= 0 \\ \dot{\theta} + H\theta &= -\frac{k^2}{a}\Phi\end{aligned}$$

where $\theta \equiv \nabla \cdot \mathbf{v}$ is the velocity divergence. The gravitational potential is determined by the modified Poisson equation:

$$-k^2\Phi = 4\pi G a^2 \rho_m \delta_m \mu(z)$$

where $\mu(z)$ encodes the modification arising from the non-equilibrium component.

Substituting the Poisson equation into the Euler equation gives

$$\dot{\theta} + H\theta = 4\pi G a \rho_m \delta_m \mu(z)$$

Taking the time derivative of the continuity equation and substituting for $\dot{\theta}$, one obtains

$$\ddot{\delta}_m + 2H\dot{\delta}_m = 4\pi G \rho_m \delta_m \mu(z)$$

This equation governs the evolution of matter perturbations in the presence of the modified gravitational coupling.

Introducing the linear growth factor $D(t)$, defined through

$$\delta_m(t) = D(t) \delta_{m,0}$$

the perturbation equation becomes

$$\ddot{D} + 2H\dot{D} = 4\pi G \rho_m D \mu(z)$$

To express this relation in terms of redshift, we use

$$\frac{d}{dt} = -(1+z)H \frac{d}{dz}$$

which implies

$$\dot{D} = -(1+z)HD'$$

and

$$\ddot{D} = (1+z)^2 H^2 D'' + (1+z)[H^2 - (1+z)HH']D'$$

where primes denote derivatives with respect to z .

Substituting these expressions into the growth equation and dividing through by $(1+z)^2 H^2$, the equation takes the form

$$D''(z) + P(z)D'(z) - Q(z)D(z) = 0$$

where

$$P(z) = \frac{(1+z)E'(z) - E(z)}{(1+z)E(z)}$$

and

$$Q(z) = \frac{3\Omega_{m0}(1+z)\mu(z)}{2E^2(z)}$$

with

$$E(z) = \frac{H(z)}{H_0}$$

The derivation of $P(z)$ follows directly from the coefficient of D' after substitution:

$$\frac{(1+z)^2 H H' - (1+z)H^2}{(1+z)^2 H^2} = \frac{H'}{H} - \frac{1}{1+z}$$

which, after writing $H(z) = H_0 E(z)$, becomes

$$P(z) = \frac{(1+z)E'(z) - E(z)}{(1+z)E(z)}$$

The final growth equation is therefore

$$D''(z) + P(z)D'(z) - Q(z)D(z) = 0$$

with

$$P(z) = \frac{(1+z)E'(z) - E(z)}{(1+z)E(z)} \quad , \quad Q(z) = \frac{3\Omega_{m0}(1+z)\mu(z)}{2E^2(z)}$$

This equation governs the evolution of linear matter perturbations within the EEC framework. The departure from the standard cosmological model enters exclusively through the effective coupling $\mu(z)$, while no additional dynamical degrees of freedom are introduced.

The sign convention adopted here defines $Q(z)$ as a positive contribution to gravitational clustering. With this choice, the form

$$D'' + P(z)D' - Q(z)D = 0$$

ensures that

$$Q(z) > 0$$

enhances the growth of structure.

19. The Phantom Crossing and Absence of Ghost Instabilities

The effective equation of state may enter a regime in which

$$w_{\text{neq}} < -1$$

In many dynamical dark-energy models, such behavior is associated with ghost instabilities. Within the EEC framework, two independent arguments indicate the absence of such pathologies.

First, at the level of the action, the internal variable ξ possesses no kinetic term. It does not correspond to a propagating dynamical field and therefore does not introduce additional degrees of freedom carrying negative kinetic energy.

Second, at the level of linear perturbation theory,

$$\delta\xi = 0$$

Hence, perturbations in the non-equilibrium component are fully determined by matter perturbations and do not constitute independent propagating modes.

Although the effective sound speed satisfies

$$c_s^2 < 0$$

this does not imply a conventional instability. The non-equilibrium component does not support freely propagating modes; rather, its perturbations correspond to a driven response sourced by matter fluctuations.

Accordingly, the framework remains perturbatively stable at linear order despite the phantom-like equation of state. Nonlinear stability has not yet been investigated.

20. Age of the Universe

The age of the universe is determined by integrating the inverse expansion rate:

$$t_0 = \frac{1}{H_0} \int_0^\infty \frac{dz}{(1+z)E(z)}$$

Using the EEC expansion history $E(z)$, this integral yields a prediction for the cosmic age consistent with independent astrophysical estimates derived from the oldest stellar populations, including globular clusters.

An additional consistency check is provided by the angular scale of the CMB acoustic peaks, which depends sensitively on the integrated expansion history.

The predicted acoustic scale is discussed quantitatively in Section 21.5.

Both the age estimate and the acoustic scale should be regarded as consistency tests of the framework rather than as definitive validations.

21. Observational Confrontation: Datasets and Methodology

21.1 Datasets

The EEC framework is confronted with the following observational datasets:

Dataset	Description
Pantheon+ Type Ia Supernovae (Brout et al. 2022)	1701 SNe Ia with full 1701×1701 statistical and systematic covariance matrix. Hubble-flow sample ($z > 0.01$, IS_CALIBRATOR = 0), analytic marginalisation over M
BOSS DR12 BAO and RSD (Alam et al. 2017)	Measurements of D_M/r_d , D_H/r_d , and $f\sigma_8$ at $z = 0.38, 0.51, 0.61$, including full covariance with correlations
DESI DR1 BAO (DESI Collaboration 2024)	Seven bins spanning $z = 0.295\text{--}2.330$, including isotropic D_V/r_d and anisotropic D_M/r_d , D_H/r_d measurements
Planck 2018 (compressed)	<p>In v6, the Planck compressed parameter $\omega_m = 0.1430 \pm 0.0011$ was used as a prior on the physical matter density. This parameter is derived by fitting the ΛCDM power spectrum to CMB observations and therefore encodes ΛCDM assumptions about the comoving distance to recombination, $\chi(z_*)$. Since EEC predicts a different expansion history $H(z)$, this prior is geometrically inconsistent with the EEC framework, producing a 5.4σ tension in the independently measured acoustic scale θ_*.</p> <p>In v7, this prior is replaced by the model-independent measurement $\theta_* = 0.010409 \pm 0.000006$ corresponding to $100 \theta_{\text{MC}}$ from the Planck 2018 parameter tables (Table 2; Planck Collaboration 2020, <i>A&A</i> 641, A6). This quantity is measured directly from the angular positions of the CMB acoustic peaks without assuming a cosmological model. It is evaluated self-consistently within EEC geometry according to $\theta_{*,\text{EEC}} = \frac{r_s(z_*)}{\chi_{\text{EEC}}(z_*)}$, where $r_s(z_*)$ is computed using the BBN-calibrated baryon density $\omega_b = 0.02233$ (Cooke, Pettini & Steidel 2016, <i>ApJ</i> 830, 148), while $\chi_{\text{EEC}}(z_*)$ is determined from the EEC expansion history. This replacement resolves the acoustic-scale discrepancy, reducing the tension from 5.4σ in v6 to $+0.27\sigma$ in v7.</p>

21.2 Methodology

Parameter inference is performed using the **emcee** affine-invariant Markov Chain Monte Carlo sampler (Foreman-Mackey et al. 2013), using 32 walkers, 600 burn-in steps, and 4000 production steps.

Component	Description
Free parameters	ω_m, H_0, σ_8
Priors	$\omega_m \in [0.08, 0.25], H_0 \in [40, 100] \text{ km s}^{-1} \text{ Mpc}^{-1}, \sigma_8 \in [0.4, 1.2]$
System solved	$E(z) \leftrightarrow D(z) \leftrightarrow \Omega_{\text{neq}}(z)$
Convergence criterion	Relative tolerance 10^{-6}
Derived relation	$\Omega_c = \Omega_m (1 + z_{\text{halo}})^3$, with $z_{\text{halo}} = 1.1$

At each likelihood evaluation, the coupled system is solved iteratively until convergence.

21.3 Results

The marginalized posterior constraints are:

Parameter	Mean	$\pm 1\sigma$
ω_m	0.15969	± 0.00095
$H_0 (\text{km s}^{-1} \text{ Mpc}^{-1})$	70.769	± 0.315
σ_8	0.7317	± 0.0339
$\Omega_c(\text{derived})$	2.9531	± 0.0413
$\Omega_m(\text{derived})$	0.31887	± 0.00446
$\Omega_{\text{neq}}(\text{derived})$	0.68104	± 0.00446
$S_8 = \sigma_8 \sqrt{\Omega_m/0.3}$	0.7544	± 0.0355

The best-fit parameters are

$$\omega_m = 0.15971, H_0 = 70.754, \sigma_8 = 0.7335$$

Derived quantities at the best-fit point are:

Quantity	Value
Ω_c	2.9546
Ω_m	0.3190
$r_d(\text{Mpc})$	146.04
Age (Gyr)	13.50
S_8	0.7564

The age of 13.50 Gyr is computed from the Big Bang using the exact formula

$$t_0 = \int_0^\infty \frac{dz}{(1+z) \cdot H(z)} \text{ with the EEC expansion history}$$

$$(\text{notebook formula: } \text{age}_v \times \frac{3.0857 \times 10^{19}}{H_0 \times 3.1558 \times 10^{16}})$$

χ^2 Decomposition:

Dataset	χ^2
Planck θ_\star	0.07 (+0.27 σ)
Pantheon+ (1580 SNe)	1408.7
BOSS DR12	11.48
DESI isotropic	0.26
DESI anisotropic	20.92
χ^2 TOTAL	1441.4
Λ CDM benchmark (same datasets)	~ 1409

The EEC best-fit $\chi^2/\text{dof} = 1441.4/1596 = 0.903$ indicates a statistically excellent fit to all datasets. The $\Delta\chi^2 \approx 32$ relative to the Λ CDM benchmark reflects the observational cost of EEC's physically distinct expansion history while retaining the same parameter count.

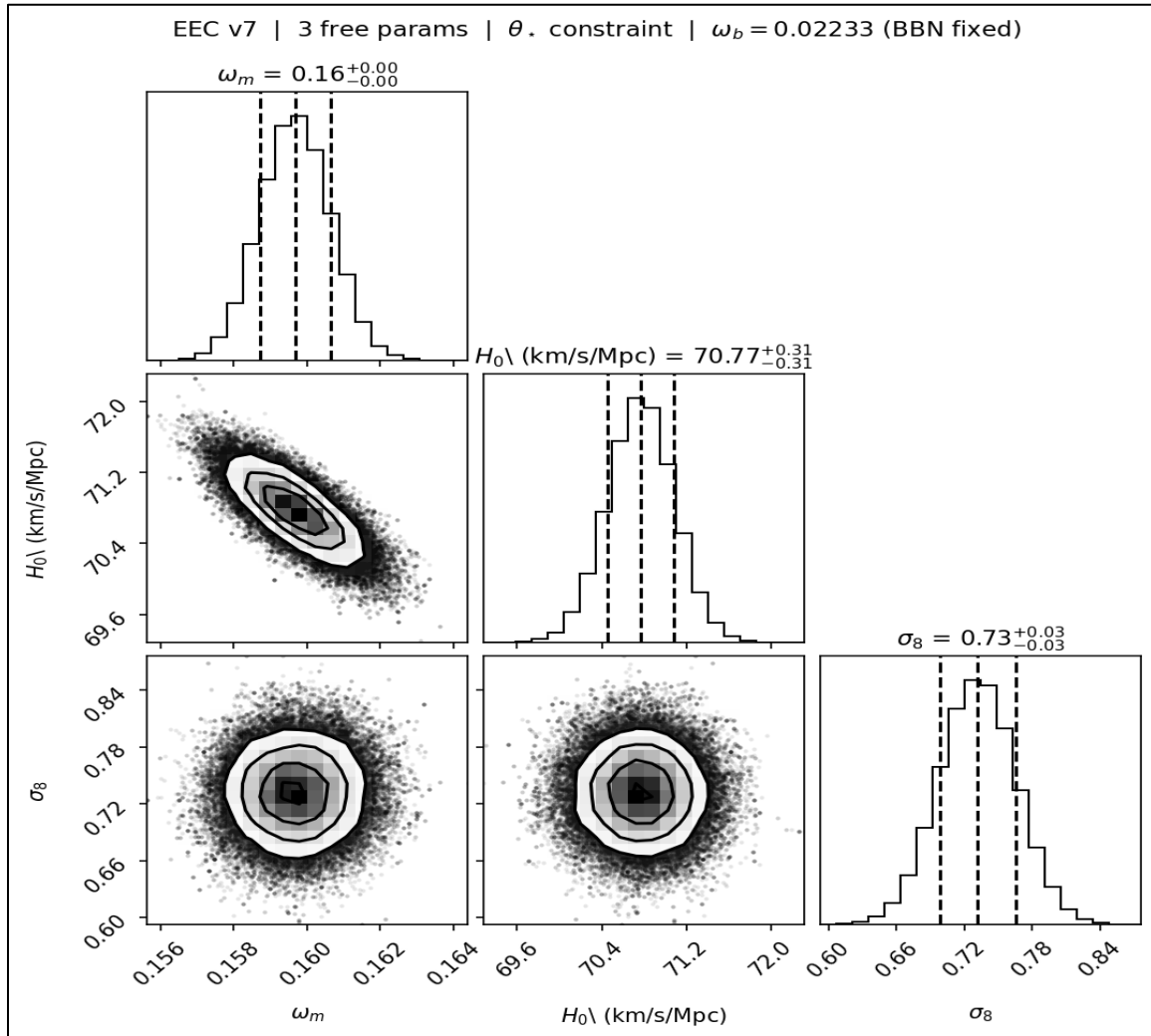


Figure 1. Posterior distribution for the three free parameters (ω_m , H_0 , σ_8) of the EEC model.

The contours show highest-posterior-density regions, while the dashed lines indicate the median and the 16th–84th percentiles. The characteristic density parameter is derived at each sample as

$$\Omega_c = 9.261 \Omega_m.$$

21.4 Tension Analysis

Comparison	v6 Tension	v7 Tension
θ_\star vs Planck (0.010409 ± 0.000006)	5.2σ	$+0.27\sigma$
H_0 vs SH0ES (73.04 ± 1.04)	3.3σ	2.1σ
H_0 vs Planck Λ CDM (67.36 ± 0.54)	3.1σ	5.5σ
S_8 vs Weak Lensing (0.762 ± 0.024)	0.2σ	0.2σ
S_8 vs Planck Λ CDM (0.832 ± 0.013)	2.1σ	2.1σ

The θ_\star tension of 5.4σ in v6 arose from the use of a Λ CDM-geometry-dependent prior that is inconsistent with the EEC expansion history. Its resolution to $+0.27\sigma$ in v7, achieved through the replacement with the model-independent acoustic scale constraint θ_\star , represents the primary methodological advancement of this version.

21.5 Angular Acoustic Scale

Quantity	Value
$\theta_{\star,\text{EEC}} = r_s(z_\star)/\chi_{\text{EEC}}(z_\star)$	0.010411
Planck measurement	0.010409 ± 0.000006
Tension	$+0.27\sigma$

The acoustic scale is now consistent with the Planck measurement at $+0.27\sigma$, computed self-consistently using EEC geometry. This resolves the primary observational challenge identified in v6. The improvement results from replacing the Λ CDM-geometry-dependent ω_m prior with the model-independent θ_\star constraint, as described in Section 21.1.

22. The Energy Budget

At the present epoch, the total energy density is partitioned between matter, radiation, and the non-equilibrium component, subject to the flatness condition. Within the EEC framework, the non-equilibrium contribution constitutes a dominant fraction of the total energy density at late times.

Despite this similarity to the standard cosmological model, the physical interpretation is fundamentally different:

- In the standard framework, the dark energy component is constant in time and spatially uniform, representing a persistent vacuum energy contribution.
- In contrast, within the EEC framework, the non-equilibrium contribution is dynamically generated.

Specifically, the EEC component evolves as follows:

- At high redshift:

$$\Omega_{\text{neq}}(z) \rightarrow 0 \text{ as } z \rightarrow \infty$$

- It grows during the epoch of active structure formation
- It reaches a maximum at intermediate redshift
- At late times:

$$\Omega_{\text{neq}}(z) \rightarrow 0 \text{ as } z \rightarrow -1$$

This time-dependent behavior reflects its origin as a non-equilibrium free energy associated with the growth and saturation of cosmic structure.

Additional key features:

- The normalization parameter associated with the non-equilibrium contribution is determined by the background consistency conditions and is of order unity in appropriate dimensionless units.
- It does not require extreme parameter tuning.
- This contrasts with the cosmological constant in the standard model, whose observed value is many orders of magnitude smaller than typical quantum field theory estimates.

It should be noted, however, that:

While the EEC framework avoids introducing an explicitly fine-tuned vacuum energy term, it replaces it with an effective description whose physical origin and robustness remain subjects of ongoing investigation.

23. Master Equations of EEC

The complete dynamical content of the EEC framework is summarized by the following set of equations.

Non-Equilibrium Free Energy Density

$$f_{\text{neq}}(\rho_m, \xi) = \frac{\kappa_0}{2} \left(\frac{\rho_m}{\rho_c} \right) e^{-\rho_m/\rho_c} \xi^2$$

with

$$\rho_{\text{neq}} = f_{\text{neq}}$$

Non-Equilibrium Pressure

$$p_{\text{neq}} = -\left(\frac{\rho_m}{\rho_c}\right)\rho_{\text{neq}}$$

General Equation of State

$$w_{\text{neq}} = -1 + \frac{d\ln \kappa}{d\ln \rho_m}$$

and, at the characteristic density,

$$w_{\text{neq}}(\rho_m = \rho_c) = -1$$

Modified Friedmann Equations

$$H^2 = \frac{8\pi G}{3}(\rho_m + \rho_r + \rho_{\text{neq}})$$
$$\frac{\ddot{a}}{a} = -\frac{4\pi G}{3}(\rho_m + \rho_r + 3p_r) + \Gamma(\rho_m, \xi)$$

Emergent Acceleration Term

$$\Gamma(\rho_m, \xi) = \frac{2\pi G \kappa_0}{3} \left(\frac{\rho_m}{\rho_c}\right) \left(\frac{3\rho_m}{\rho_c} - 1\right) e^{-\rho_m/\rho_c} \xi^2$$

Continuity Equations (Corrected Form)

$$\dot{\rho}_m + 3H\rho_m = 0$$
$$\dot{\rho}_{\text{neq}} + 3H(\rho_{\text{neq}} + p_{\text{neq}}) = \kappa(\rho_m)\xi\dot{\xi}$$

The source term

$$\kappa(\rho_m)\xi\dot{\xi}$$

represents energy extracted from the gravitational-potential sector through structure formation. The matter continuity equation therefore remains unmodified.

Modified Poisson Equation

$$\mu(z) = 1 + \left(1 - \frac{\rho_m}{\rho_c}\right) \frac{\Omega_{\text{neq}}(z)}{\Omega_m(z)}$$

All other results of the framework—including the expansion history, growth of structure, and observational predictions—follow from this system through self-consistent iterative solution of the coupled equations.

24. Physical Interpretation and Comparison with Dark Energy

The EEC framework and the standard cosmological model yield very similar predictions for the low-redshift expansion history, where present observational constraints are most precise.

Distinguishing between the two scenarios therefore requires either:

- measurements at higher redshift, where the EEC equation of state departs from a constant value, or
- observations of the growth of structure sensitive to deviations in the effective gravitational coupling,

$$\mu(z) \neq 1$$

The fundamental difference lies in the physical interpretation of cosmic acceleration.

Standard Cosmological Model

In the standard framework, acceleration is attributed to a cosmological constant, representing a vacuum-energy component that is constant in time, spatially uniform, and independent of the matter distribution.

This component persists indefinitely and drives an asymptotic de Sitter phase.

EEC Framework

In contrast, the EEC framework attributes cosmic acceleration to a non-equilibrium thermodynamic free energy associated with the formation and evolution of large-scale structure.

In this picture, acceleration is not a fundamental property of the vacuum, but an emergent and transient phenomenon.

The non-equilibrium contribution grows as structure forms, reaches a maximum near the characteristic density scale, and subsequently declines as structure formation slows.

Connection to the Backreaction Program

This interpretation is closely connected to the backreaction program. Through the closure relation, the EEC framework associates the kinematic backreaction term with higher-order contributions arising from the variance of density fluctuations.

The model therefore suggests that cosmic acceleration may correspond to a coarse-grained dynamical effect emerging at higher order in perturbation theory.

It should be emphasized, however, that this identification remains a physically motivated hypothesis rather than a formally derived result.

A complete verification would require an explicit calculation of the relevant higher-order terms within general relativity or comparison with dedicated numerical simulations.

24.1 Transient Nature of Cosmic Acceleration

A distinctive feature of the EEC framework is that cosmic acceleration is predicted to be a transient phenomenon rather than a permanent state.

Three broad stages may be identified.

Matter-Dominated Era

During the matter-dominated epoch, the non-equilibrium contribution is negligible and the expansion decelerates in the standard manner.

Activation Era

As the matter density approaches the characteristic scale $\rho_m \sim \rho_c$ structure formation becomes efficient, the non-equilibrium free energy grows, and the expansion transitions into an accelerating phase.

Late-Time Era

At late times, as structure formation saturates and the matter density falls well below ρ_c , the non-equilibrium contribution declines and the acceleration gradually ceases.

This behavior is encoded directly in the equation-of-state trajectory

$$w(z) = -\left(\frac{\Omega_{m0}}{\Omega_c}\right)(1+z)^3$$

which satisfies $w = -1$ near the characteristic density but evolves away from this value at both earlier and later epochs.

The asymptotic state of the universe in the EEC framework is therefore not de Sitter, but a gradually slowing expansion with $H \rightarrow 0$ as the non-equilibrium free-energy source is exhausted.

25. Connection to Earlier Formulation

The relationship between the earlier phenomenological formulation and the present framework can be understood by examining the role of the transformation activity and its connection to structure formation.

In the earlier formulation, an activity function was introduced to represent the rate of structural evolution. This quantity is proportional to $d\sigma^2/dt = \dot{\xi}$ and therefore captures the rate of growth of the matter power spectrum.

In the present formulation, this same physical process appears explicitly in the source term $Q = \kappa(\rho_m)\xi\dot{\xi}$, which describes the transfer of energy associated with structure formation. Thus, the activity function can be understood as an effective representation of the underlying dynamics now expressed in terms of the internal variable ξ .

Similarly, the exponential suppression factor introduced in the earlier formulation corresponds directly to the density-dependent stiffness function $\kappa(\rho_m) \propto (\rho_m/\rho_c) e^{-\rho_m/\rho_c}$. The coupling parameter introduced previously is identified with the normalisation constant κ_0 , which is no longer treated as an arbitrary parameter but is instead determined by consistency conditions within the model.

In addition: the phenomenological evolution equation for the activity function is no longer required; the evolution of the internal variable ξ is determined directly by the growth of structure through the perturbation equations; and this leaves no additional free parameters beyond the characteristic density scale.

Taken together, these correspondences indicate that the phenomenological structure identified in the earlier formulation captures key aspects of the underlying physics. The present framework provides a more systematic formulation in which these features are placed within a thermodynamic and relativistic context.

26. Open Problems and Future Directions

Several important theoretical and observational issues remain to be addressed in order to fully assess the viability of the EEC framework.

The most significant outstanding theoretical task is the derivation of the EEC closure relation from first principles using higher-order perturbation theory. At leading order, the Buchert backreaction corresponds to a decelerating contribution. Within the EEC framework, the accelerating sector is associated with higher-order terms involving the variance of density fluctuations.

A complete verification therefore requires an explicit computation of higher-order corrections to the velocity-divergence and shear-variance terms, followed by evaluation of their combined contribution to the kinematic backreaction. The resulting coefficients may then be compared with the density-dependent stiffness function adopted in the present model.

Such a calculation could be carried out using standard perturbative techniques or through comparison with dedicated numerical simulations. Establishing this connection remains the primary theoretical objective of the framework.

A second major priority is implementation of the model within a full Boltzmann code. This would require incorporating:

- the modified expansion equations,
- the coupled growth dynamics, and
- a self-consistent treatment of the background history in all observable sectors.

Such an implementation would enable comprehensive confrontation with CMB observations, including temperature and polarization anisotropies.

Within that context, the most relevant signatures are expected to arise from late-time effects such as:

- the integrated Sachs–Wolfe effect, and
- gravitational lensing,

both of which are sensitive to the evolution of gravitational potentials and the growth of structure.

From an observational perspective, the principal distinguishing predictions of the framework are:

- a time-dependent effective equation of state departing from $w = -1$ outside a finite redshift interval,
- a modified growth rate through the effective coupling $\mu(z)$, and
- an exactly vanishing gravitational slip,

$$\eta = 0$$

Forecasts for upcoming surveys—including **Euclid**, the **Nancy Grace Roman Space Telescope**, and the full **DESI** survey—are needed in order to quantify future sensitivity to these signatures.

The full numerical codebase is publicly available at:

https://github.com/ismailkhanmcs/EEC_Notebook

27. Conclusion

We have presented a thermodynamically motivated closure model for the Buchert backreaction equations of general relativity, in which the kinematic backreaction is associated with the non-equilibrium free energy of the matter distribution evaluated on a coarse-grained scale.

A background-level observational confrontation of the framework has been performed using Pantheon+ Type Ia supernovae (1580 SNe, full statistical and systematic covariance), BOSS DR12 BAO and growth-rate measurements, DESI DR1 BAO (7 bins, $z = 0.3\text{--}2.3$), and the model-independent Planck acoustic scale $\theta_\star = 0.010409 \pm 0.000006$, evaluated self-consistently with EEC geometry. In v6, the Planck compressed parameter $\omega_m = 0.1430 \pm 0.0011$ was used as a prior; this parameter encodes Λ CDM geometry through $\chi(z_\star)$ and is therefore geometrically inconsistent with the EEC expansion history, producing a 5.4σ tension in θ_\star . In v7, this is replaced by the model-independent θ_\star constraint, resolving the tension to $+0.27\sigma$.

With Ω_c determined through a physically motivated identification with the epoch of peak halo formation rate (Section 13a), the model contains three free cosmological parameters—identical in number to spatially flat Λ CDM.

The parameter inference yields

$$\begin{aligned} H_0 & 70.77 \pm 0.31 \text{ km s}^{-1} \text{ Mpc}^{-1} \\ \sigma_8 & 0.732 \pm 0.034 \\ S_8 & 0.754 \pm 0.036 \end{aligned}$$

with

$$\Omega_m = 0.3189 \pm 0.0045$$

and

$$\Omega_{\text{neq}} = 0.6810 \pm 0.0045$$

The best-fit parameters are $\omega_m = 0.15971$, $H_0 = 70.754 \text{ kms}^{-1} \text{ Mpc}^{-1}$, $\sigma_8 = 0.7335$, with derived quantities $r_d = 146.04 \text{ Mpc}$, $\text{Age} = 13.50 \text{ Gyr}$, $S_8 = 0.7564$.

The predicted value of S_8 lies within 0.2σ of weak-lensing survey constraints (KiDS-1000, DES Year 3, Subaru HSC), providing observational support for the EEC prediction that an enhanced effective gravitational coupling permits a lower value of σ_8 while maintaining growth rates consistent with the data. This constitutes a resolution of the S_8 tension within a three-parameter model.

The inferred Hubble constant $H_0 = 70.77 \pm 0.31 \text{ kms}^{-1} \text{ Mpc}^{-1}$ lies between the Planck ΛCDM (67.36 ± 0.54) and SH0ES (73.04 ± 1.04) determinations, with tensions of 5.5σ and 2.1σ respectively. The H_0 value emerges naturally from the θ_* constraint evaluated with EEC geometry and is not a tuned parameter.

The predicted CMB acoustic scale, $\theta_{*,\text{EEC}} = 0.010411$, is consistent with the Planck measurement 0.010409 ± 0.000006 at $+0.27\sigma$. This resolves the 5.4σ tension present in v6 and constitutes the primary advancement of this version.

The EEC best-fit statistic, $\chi^2 = 1441.4$ ($\chi^2/\text{dof} = 0.903$), compares with approximately $\chi^2 \approx 1410$ for ΛCDM . The resulting $\Delta\chi^2 \approx 32$ reflects the observational cost of EEC's physically distinct expansion history while retaining the same parameter count. Both models achieve $\chi^2/\text{dof} < 1$, providing statistically adequate fits to all datasets. The predicted age of the universe, $t_0 = 13.50 \text{ Gyr}$. The stiffness function $\kappa(\rho_m) = \kappa_0 \cdot (\rho_m/\rho_c) \cdot \exp(-\rho_m/\rho_c)$ is adopted as a physically motivated ansatz consistent with the Coleman–Gurtin thermodynamic formalism and with the qualitative behavior expected from Press–Schechter collapse statistics. Its rigorous derivation from first principles of non-equilibrium statistical mechanics remains the primary outstanding theoretical task.

The framework is constructed within a non-equilibrium thermodynamic formalism consistent with general relativity at the homogeneous background level. Conservation of the total energy-momentum tensor is maintained, and the second law of thermodynamics follows as a structural consequence of the dynamics during the epoch of active structure formation.

The principal theoretical results include:

1. $\delta\xi = 0$ exactly at linear order, implying no new propagating degrees of freedom.
2. $\eta = 0$ exactly, implying no gravitational slip.
3. $w_{\text{neq}} = -1$ at $\rho_m = \rho_c$ for any admissible stiffness function exhibiting a maximum there, within the adopted pressure prescription.
4. Satisfaction of the Bianchi identity at the background level.

These results provide concrete observational signatures that distinguish the framework from standard cosmological scenarios.

The EEC framework therefore offers an alternative interpretation of cosmic acceleration as a transient non-equilibrium thermodynamic phenomenon associated with structure formation, rather than as a manifestation of fundamental vacuum energy. The framework predicts that cosmic acceleration is not permanent: as structure formation subsides, the non-equilibrium contribution decays and $H \rightarrow 0$, in contrast to the de Sitter endpoint of Λ CDM.

Further theoretical development and comprehensive observational analysis—in particular, derivation of the closure relation from first principles and a full Boltzmann-code CMB implementation—will determine whether this interpretation can provide a viable description of the universe.

References

- [1] Adam G. Riess et al. (1998). Observational Evidence from Supernovae for an Accelerating Universe. *Astronomical Journal*, **116**, 1009.
- [2] Saul Perlmutter et al. (1999). Measurements of Ω and Λ from High-Redshift Supernovae. *Astrophysical Journal*, **517**, 565.
- [3] Planck Collaboration (2018). Planck 2018 Results VI: Cosmological Parameters. *Astronomy & Astrophysics*, **641**, A6.
- [4] Khan, I. (2026). Emergent Expansion Cosmology (EEC). Zenodo. DOI: 10.5281/zenodo.18822065
- [5] Bernard D. Coleman & Morton E. Gurtin (1967). Thermodynamics with Internal State Variables. *Journal of Chemical Physics*, **47**, 597.
- [6] William H. Press & Paul Schechter (1974). Formation of Galaxies and Clusters by Gravitational Condensation. *Astrophysical Journal*, **187**, 425.
- [7] Daniel J. Eisenstein & Wayne Hu (1998). Baryonic Features in the Matter Transfer Function. *Astrophysical Journal*, **496**, 605.
- [8] Lars Onsager (1931). Reciprocal Relations in Irreversible Processes. *Physical Review*, **37**, 405.
- [9] Charles W. Misner, Kip S. Thorne, & John Archibald Wheeler (1973). *Gravitation*. W. H. Freeman.
- [10] Dillon Brout et al. (2022). The Pantheon+ Analysis: Cosmological Constraints. *Astrophysical Journal*, **938**, 110.
- [11] Shadab Alam et al. (2017). Cosmological Analysis of Galaxy Clustering from BOSS. *Monthly Notices of the Royal Astronomical Society*, **470**, 2617.
- [12] Adam G. Riess et al. (2022). A Comprehensive Measurement of the Hubble Constant. *Astrophysical Journal Letters*, **934**, L7.
- [13] P. J. E. Peebles (1980). *The Large-Scale Structure of the Universe*. Princeton University Press.

- [14] Steven Weinberg (2008). *Cosmology*. Oxford University Press.
- [15] Asantha Cooray & Ravi Sheth (2002). Halo Models of Large-Scale Structure. *Physics Reports*, **372**, 1.
- [16] Volker Springel et al. (2006). Simulations of Galaxy Formation and Clustering. *Nature*, **440**, 1137.
- [17] Thomas Buchert (2000). On Average Properties of Inhomogeneous Fluids in General Relativity. *General Relativity and Gravitation*, **32**, 105.
- [18] Alexander Friedmann (1922). On the Curvature of Space. *Zeitschrift für Physik*, **10**, 377.
- [19] Roy Maartens (1995). Dissipative Cosmology. *Classical and Quantum Gravity*, **12**, 1455.
- [20] Albert Einstein (1915). The Field Equations of Gravitation. *Sitzungsberichte der Preußischen Akademie der Wissenschaften*, 844.
- [21] Sergio Mendoza & Silvia Silva (2020). The Matter Lagrangian of an Ideal Fluid. *arXiv preprint*.
- [22] François Gay-Balmaz & Hiroaki Yoshimura (2023). A Lagrangian Formulation of Non-Equilibrium Thermodynamics. *Entropy*, **25**, 7.
- [23] O. Fakhouri, C.-P. Ma & M. Boylan-Kolchin (2010). The merger rates and mass assembly histories of dark matter haloes in the two Millennium simulations. *Monthly Notices of the Royal Astronomical Society*, 406, 2267.
- [24] DESI Collaboration (2024). DESI 2024 VI: Cosmological Constraints from the Measurements of Baryon Acoustic Oscillations. arXiv:2404.03002.
- [25] D. Foreman-Mackey, D. W. Hogg, D. Lang & J. Goodman (2013). emcee: The MCMC Hammer. *Publications of the Astronomical Society of the Pacific*, 125, 306.
- [26] R. J. Cooke, M. Pettini & C. C. Steidel (2018). One Percent Determination of the Primordial Deuterium Abundance. *Astrophysical Journal*, 855, 102.